

Strain-cum-Deformation Analysis of Friction Stir Welded AA5052 and AA6061 Samples with Microstructural Analysis

T. Prabakaran¹, M.B.S. Sreekara Reddy², A. Bovas Herbert Bejaxhin^{3*}, Ramanan⁴, Pothamsetty Kasi V⁵ and jenaris⁶

¹ Department of Mechanical Engineering, St. Peters University, Chennai 600 054, Tamil Nadu, India.

E-mail: prabaezhile1977@gmail.com

² Department of Mechanical Engineering, Lakireddy Bali Reddy College of Engineering, Mylavaram, 521230, AP, India.

^{3*} Associate Professor, Department of Mechanical Engineering, Saveetha School of Engineering, SIMATS, Chennai.

E-mail: herbert.mech2007@gmail.com

⁴ Department of Mechanical Engineering, PSN Engineering College, Tirunelveli, Tamilnadu, India.

E-mail: ramananinjs2020@gmail.com

⁵ Department of Mechanical Engineering, Koneru Lakshmaiah Education Foundation, Vaddeswaram, AP, India.

⁶ Department of Mechanical Engineering, PSN Engineering College, Tirunelveli, Tamilnadu, India.

Abstract

Friction stir welding is a brand-new welding technique that was discovered in 1991 by Wayne Thomas in United Kingdom. It is a form of solid state welding in which a non-consumable electrode is used to unite two work components without melting either of them. The mechanical characteristics and numerous microscopic studies of materials used for friction stir welding, such as duplex stainless steel UNS S31803, SA 213 tube to SA387, Al7075 alloy, and AA6061 metal, are reviewed. Here, welded areas were the primary focus of the microscopic study, and the diverse outcomes are also discussed.

Keywords: Friction Stir Welding, Duplex Stainless steel, PDZ, ERD, FWTPET

1.0 Introduction

To create a single construction at the dawn of human history, it was crucial to combine two elements. When compared to a combination of identical metals, dissimilar metals typically boost the material's mechanical qualities for the majority of uses in our daily lives [4]. By using standard welding techniques like arc welding, gas welding, etc., these metals cannot be welded [3]. Wayne Thomas of TWI therefore created a traditional welding technique in 1991 to join the two different metals [1]. Al alloys are often divided the two

groups: able to be heated alloys and alloys that cannot be heated. Heat-treatable alloys can be strengthened using a variety of heat treatments, whereas alloys that cannot be strengthened through heat treatment using heat treatments.

The conventional method of strengthening these non-heat treatable alloys is to combine several alloying metals, also referred to as composites. The welding capabilities of high strength alloys are lower. The alloy Al7075, which has a high ratio of strength to weight, belongs to the group of alloys mentioned above. Due to the presence of specific precipitates as Mg₂Zn and Al₂CuMg, this alloy has less

*Corresponding author

favourable welding properties. These cause the welded area to crack, which also decreases the weld's effectiveness [5]. Duplex stainless steel is a member of a family of steels with superior weldability and good corrosion resistance.

DSS (duplex stainless steels) is a material that is used in a variety of industries, including the chemical sector, offshore business, nuclear power plants, and structural uses. Despite having higher welding capabilities, this DSS (duplex stainless steels) has an extremely difficult joining process. However, the advancement of welding technology has improved this class of steels' capacity to weld [6]. Here, the microstructure and test-related behaviour of UNS S31803 duplex stainless steel are discussed.

Mechanical stir welding, or FSW, is a process for joining two dissimilar tubes. SA 213 tube to SA387 tube were examined, along with their microstructure and the welded tube's performance in various tests in the welded region [7]. Additionally, AA6061-T6 friction stir welded alloy's yield strength (YS), per cent elongation (%E), and ultimate tensile strength (UTS) are discussed [8].

2.0 Experimental Procedure

AL7075 alloy material welding configuration

Utilising a milling machine and power hacksaw, commercial sheets made of aluminium 7075-T651 that were cut to the necessary measurements (50 mm wide and 100 mm length). The inexpensive metal was put through tensile testing on a 50 KN programmable universal testing apparatus at standard temperature with a constant head speed of 0.5 mm/min. The the maximum tensile strength of the foundation material was found to be 568 Mpa.

The joints were constructed using non-consumable accelerated steel M2 grade tools with a pin with a cylindrical thread. Three distinct shoulder diameter tools were used during the studies, which are summarised and displayed below [Figure 2]. The mechanical evaluation (tensile testing) of the welded material came next [Table 1].

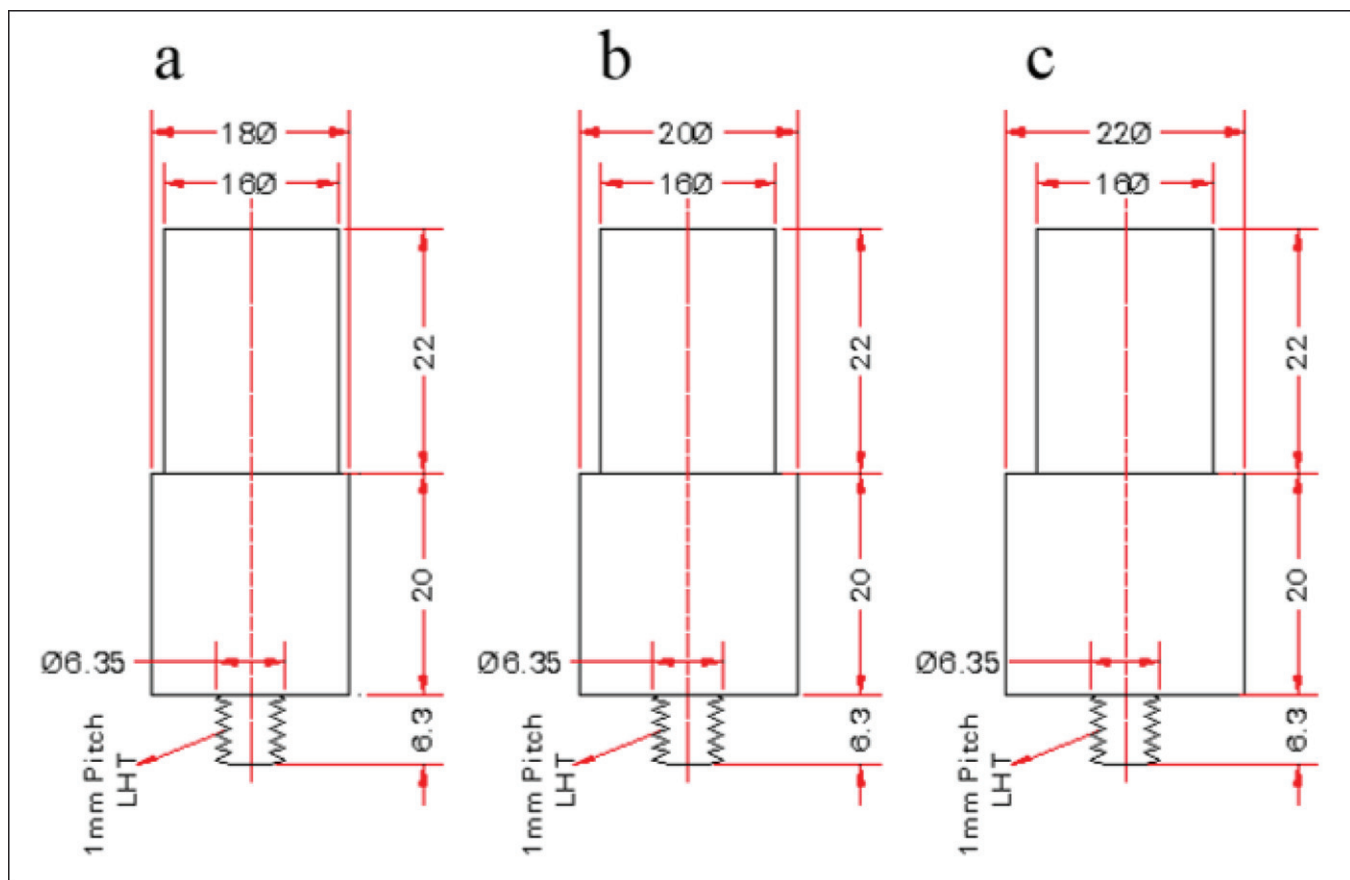


Figure 1: Measurements of the tool (a) 17mm (b) 19mm (c) shoulder diameter of 21 mm

Table 1: 2mm shoulder diameter

Example ID	Shoulder distance (in mm)	Speed of Tool Rotation (in rpm)	Speed of Tool Rotation (in mm/min)	Tilt Angle of the Tool (in degrees)	Plunge Depth of the Tool (in mm)	Worn-out thermocouples (in nos.)
S I	17	1500	50	2°	6.5	2
S II	29					2
S III	21					2
S11	17					4
S22	29					4
S33	21					4

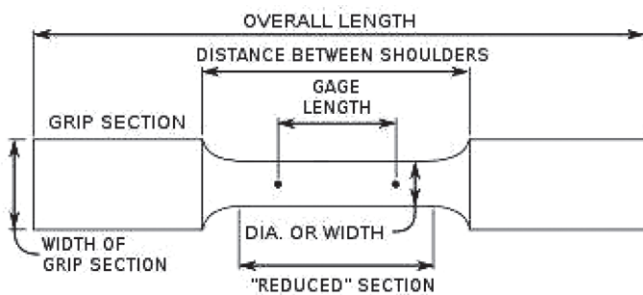


Figure 2: The common tensile specimen

Property tensile strength

After the natural ageing process, friction stir-welded aluminium alloys were put through a tensile strength test. The materials that were machined in accordance with ASTM specifications were subjected to the test. The test was run using different sets of rod diameters. The 19mm shoulder diameter weld demonstrated the weld’s maximum strength. The weld exhibited an 8.66% elongation and a maximum strength of 262MPa. The joint’s tensile strength with the 17mm diameter exhibited the lowest value, 192 MPa, while the joint with the 21mm shoulder diameter had the highest value, 242 MPa [5]. Using a power hacksaw, the welded cross section is chopped into the desired shape.

Power hacksaws are used to cut the welded connections into the desired shapes for the tensile specimens, as shown in Fig.6. The test specimens are prepared in accordance with ASTM E8M-04 rules published by the American Society for Testing of Materials. Tensile tests were performed using a universal testing apparatus from INSTRON with a 100kN load capacity (Fig.7)(a) According to ASTM requirements, the sample has been loaded at a stress level of 2mm/min, and the specimen has a connected extensometer,



Figure 3: Tensile specimen samples



Figure 4: (a) All-purpose Testing Device (b) specimen and extensometer mounted (INSTRON)

causing the tensile sample to deform as illustrated in Fig.7(b). Once necked and recording loading and displacement, the specimen ultimately fails. Evaluations have been made of the offset of 0.2% yield potency, the maximum tensile strength, and elongation percentage.

3.0 The Findings and Discussion

Tensile attributes

The yield potency, ultimate tensile power, elongation percentage, and jointly effective of FSW joints have been evaluated. Each circumstance was evaluated on two specimens, and the results are reported as the average of the two specimens' results. The tensile characteristics of the FSW joints can be deduced to be influenced by the tool pin profile and rotating speed. Regardless of rotational speed, the fifteen (5×3) joints that were made using square tool profiles and cylindrical pin profiles had better tensile qualities than the others. The analysis is carried out with a welding speed of 800 rpm using a taper tool because the tensile value was more than that.

Analysis of the microstructure

The results of the microstructure investigation performed using an optical microscope in the welded region are listed below. Below is a description of the many regions that the optical microscope identified. When compared to the advancing side, the temperatures on the receding side are a little lower. They are, respectively, 355.3°C, 358°C, and 382.7°C. Same side, different distances type configuration suggests that the weld's temperature rises in the weld's direction and toward its centre [5].

Material weld set up for the alloy AA6061-T6

To assess the tensile qualities of the joints, machined joints were welded the necessary tensile specimens in accordance with the American Society for Testing of Materials

Table 2: Results of the Taper pin set up's tensile test

Snap Pin (rpm)	Speed of Welding (mm/sec)	Tensile Power (N/mm ²)
700	40	129.620
	50	119.571
800	40	138.897
	50	128.114
900	40	96.198
	50	75.110
1000	25	75.354
	40	87.616

Table 3: Results of triangular pin set up's tensile tests

Triangular Pin (rpm)	Speed of Welding (mm/sec)	Tensile Power (N/mm ²)
700	25	107.668
	40	94.166
	50	106.289
	60	63.220
800	40	93.815
	50	108.81
	60	104.895
900	40	88.482
	50	92.505
1000	25	23.123

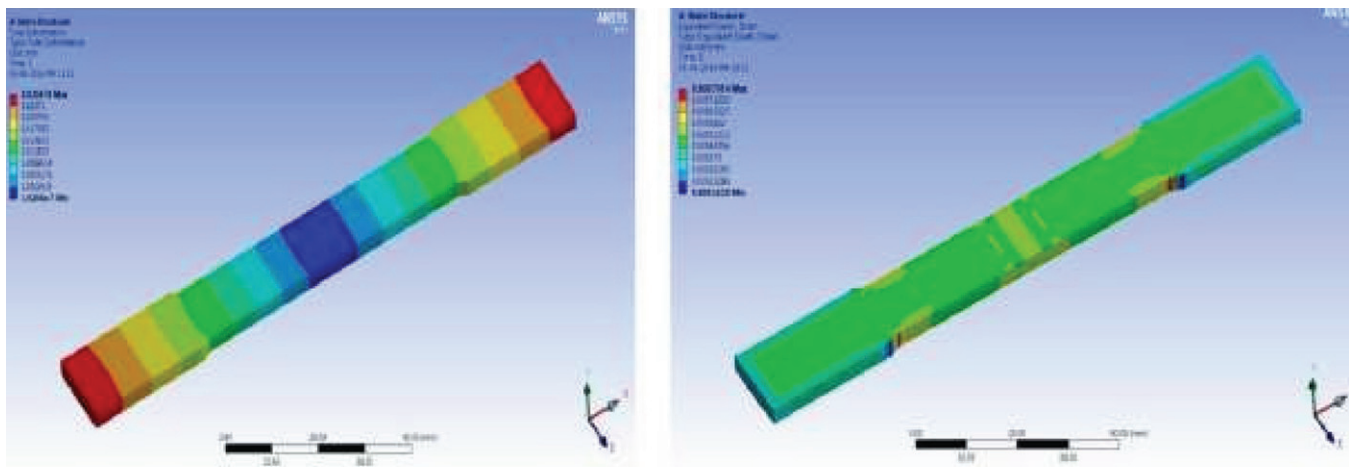


Figure 5: Analysis of deformation and strain in ANSYS

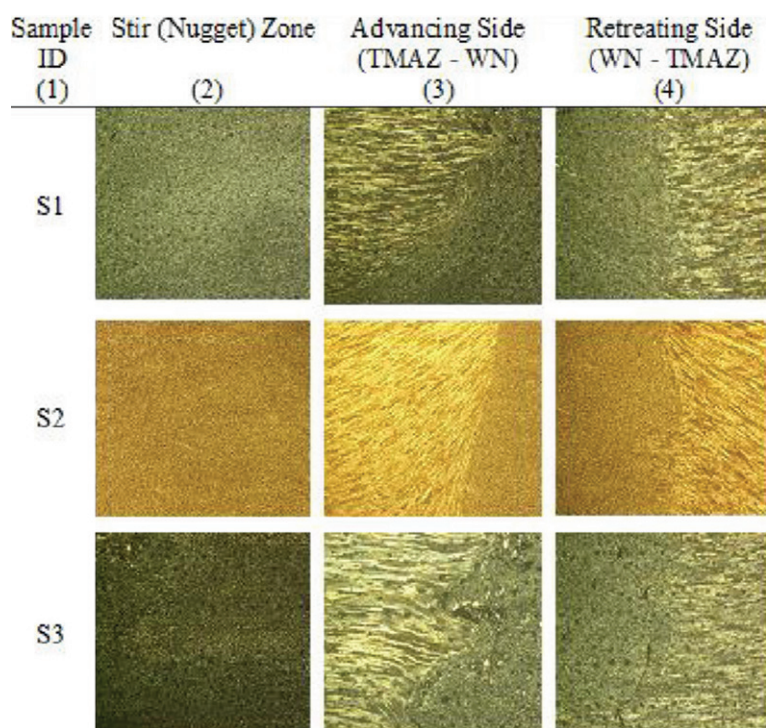


Figure 6: The welding area’s microstructure

(ASTM E8M-04) standards. Twenty joints of each alloy were made in total, as per the design matrix’s instructions, for this experiment. In Table 2 [8], the parameters of a few of the manufactured joints are shown.

4.0 The Creation of the Mathematical Model

Use of variance analysis (ANOVA) was employed to ascertain whether the generated empirical association for the response elements UTS, YS, and % E was adequate. Table 3 lists the welding with friction in an experiment parameters and their levels in the form used in this review. The fitted quadratic model is statistically significant to examine the response variables, according to the fit summary. At a 95% confidence level, it is discovered that the computed F ratios exceed the values in the table; as a result, the models are deemed adequate [8].

Table 5: Some of the manufactured joints’ characteristics

Experiment No	A: Acular Load (kN)	B: Rotational speed (rpm)	C: Traversal rate (mm/min)	UTS (Mpa)	YS (Mpa)	% E
1	8	1000	60	138	129	6.9
2	8	1000	60	142	130	7.3
3	6	800	90	135	125	4.2
4	6	1200	30	148	136	5.8
5	10	1200	90	198	178	7.2
6	10	800	60	137	130	6.2
7	8	1000	60	153	145	6.8
8	8	1000	60	159	146	5
9	6	800	60	137	130	4.8
10	8	1000	30	130	122	6.3
11	8	1200	90	145	132	6.5
12	10	1200	90	191	154	6.4
13	8	1200	60	190	159	4.5
14	6	800	30	193	151	5.5
15	10	1000	30	158	142	6.4
16	10	1000	60	163	151	6.5
17	8	1000	30	176	163	6.4
18	6	1000	60	190	159	6.5
19	8	1000	60	145	135	7.3
20	8	1000	60	140	130	7

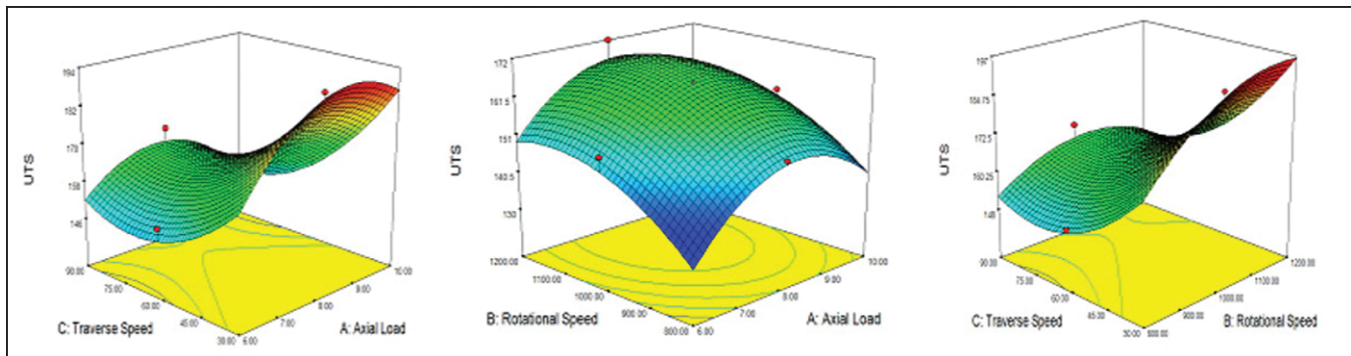


Figure 7: Response UTS of joint A-C

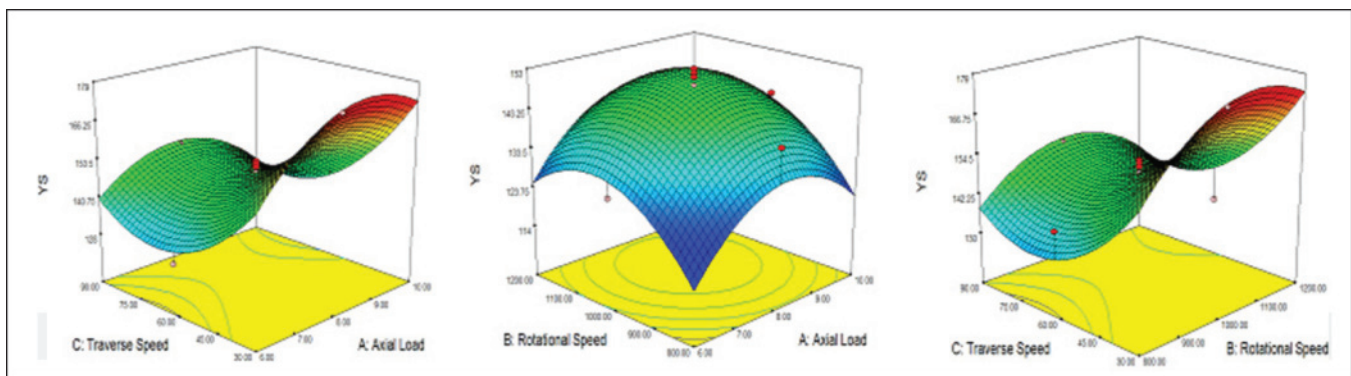


Figure 8: 3D Response YS of joint A-C

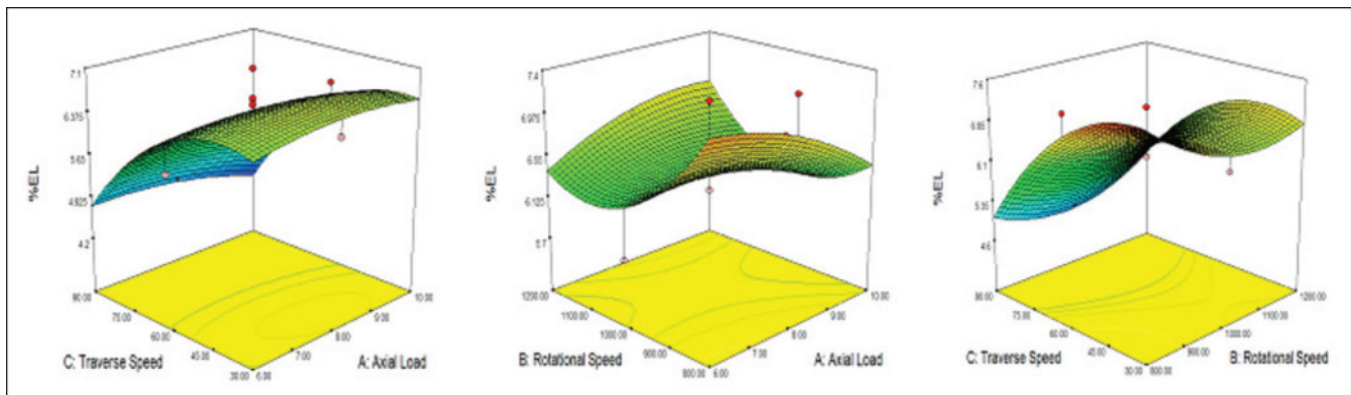


Figure 9: % Response E of joint A-C

Process Parameters' Impact on UTS (ultimate tensile strength)

In Figure 3, the plot for the joint's reaction UTS is examined and shown. This plot depicts the change in UTS (ultimate tensile strength) as each FSW parameter deviates according to the reference value and provides the response surface. The counter graphs showing the effects of any two

input parameters interacted on the UTS (ultimate tensile power) are shown in Figure 3 A–C with the other parameters at their centre level. Up to a certain point, a speed of the tool's rotation increasing and FS welded joints experience UTS due to axial force to rise; thereafter, an increase in welding speed sources the UTS to rise [8]. The interaction effect of any two input factors on the YS is shown in contour plots in Figure 3. Due to sufficient friction and material flow, the loftier rotating

speeds, slower welding rates, and loftier axial forces eliminate flaws in the welded zone of the joints, increasing YS[8].

Process parameter effects on % Elongation

The TE of the FS fused joints increases constantly as tool rotating speed and Inverse force rise, whereas selding velocity decrease causes an increase in TE. Due to sufficient friction and flow of plastic of the material, increasing the rotation speed of the tool and axial force while slowing down the welding speed results in the elimination of WZ joint flaws, which raises the TE [8].

5.0 FSW Response Optimization of parameters

One of the main goals of this work was to discover the best process variables [8] from the generated numerical model in order to maximise the UTS, YS, and % E of friction stir welded

joints of AA 6061-T6. Desirability is a multiple response technique that Derringer and Such explain. The overall desirability function, a dimensionless performance metric, is created by combining several responses using this method for solving multiple-response optimization problems. Where the desirability scales from 0 to 1 [9]. The UTS, YS, and TE that can be attained, as anticipated by the aforesaid approach, are 197.50 MPa, 175.25 MPa, and 6.96%, respectively.

Experiments on friction welding

The statistical method of experiment design is used to create the welding components under consideration. Each element will produce two degrees of freedom in the statistical approach of designing experiments, giving a total of all four parameters have eight degrees of freedom. As a result, the experimental set up must consist of at least nine experiments with a minimum of eight degrees of freedom. As a result, a L9 orthogonal array made up of nine separate sets of process parameters was created, as shown in Table 4 [6].

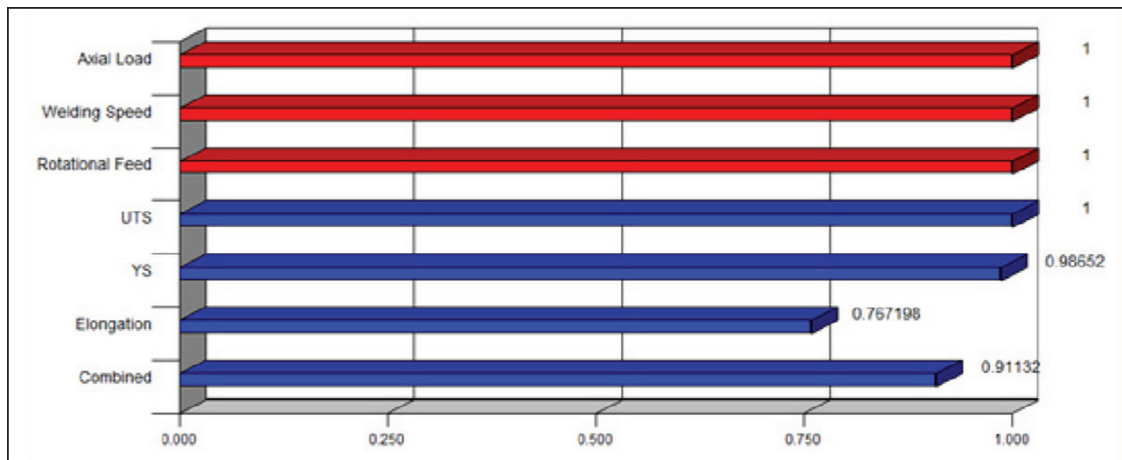


Figure 10: FSW parameters and responses

Table 6: L9 Orthogonal array

Exp. No	Warming power (Mpa)	Heating phase (sec)	Negative force (Mpa)	Unsettling situation (sec)
1	28	3	58	2
2	28	4	68	3
3	28	5	78	4
4	38	3	68	4
5	38	4	78	2
6	38	5	58	3
7	38	3	78	3
8	48	4	58	4
9	48	5	68	2

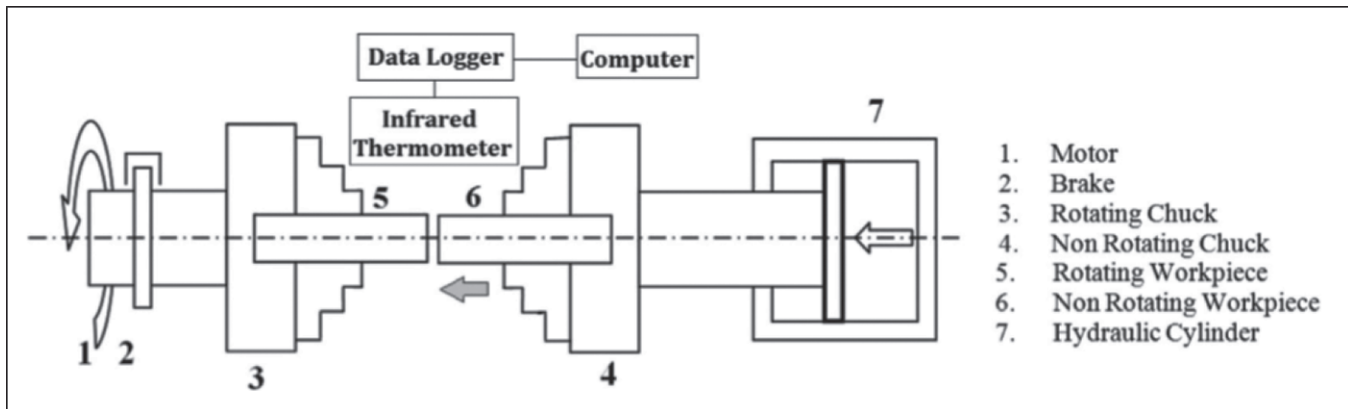


Figure 11: Experimental Environment

The friction welding equipment was used for the welding trials, and each of the work parts received a steady rate of rotation of 1500 rpm during the frictional heating process. In Figure 4 [6], the experimental set up is reviewed.

Measurement and testing

After the welds had been performed satisfactorily, the flash was taken out using machining. For the purpose of examining the weld microstructures, the samples were cut, the weld surface was polished to a 1200 size of the grit, cloth polished through 0.05 mm-sized alumina flour, and lastly etched. Microhardness A measurement was taken on the weld path's transverse track for the parent content, the ZD, and the welding metal. With an indentation load of 500g, a dwell period of 15 s, and an rate of indentation of 50mm/s, a Vickers micro hardness tester was employed.

Controlled by a non-e contact infrared thermometer and a digital data recorder were used to record experimental temperature values during the friction welding process. The testing protocols were reviewed, and the XRD analysis was performed using a best X-ray diffract metre with wavelength radiation 1.544Å [10].

General continuous drive assumptions Slipstream Welding

The heat produced and the pressure at the interface weld were presummatum to be consistent for the continuous drive friction welding analysis. In practise, the heat distribution changes along the component's radial distance from its centre line. But this supposition was made in order to prevent complexity. It was expected that the duplex stainless steel was isotropic and homogenous. This model did not take into account the Chucks at the ends of the component that holds the portion. The heat loss from convection, conduction, and radiation were taken into account in thermal boundary conditions. Calculated heat generation was provided at the weld interface. In order to account for heat losses, the analysis used a 0.4 material emissivity and a 25 W/m²-K temperature-transfer efficiency. In Figure 12, the boundary conditions are shown in detail.

Boundary circumstances

Nodes on the exterior of a unrotating element that are similar to the contact surface are entirely restricted during friction

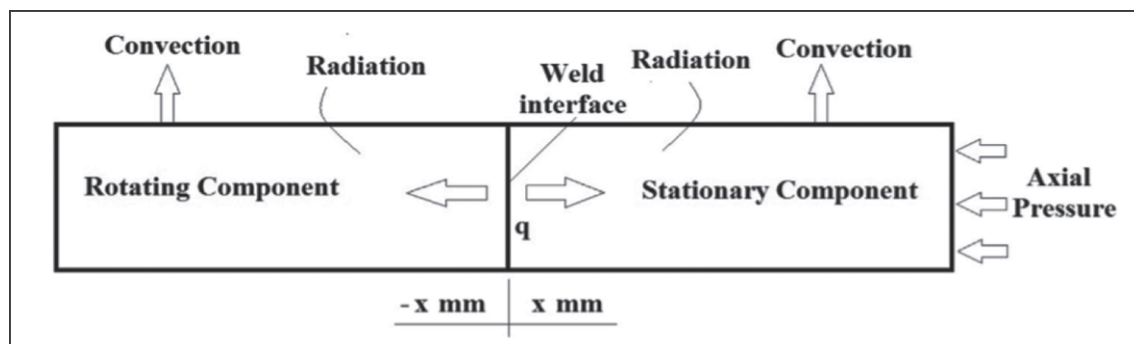


Figure 12: Specific Boundary Requirements

Table 7: PM, WA, and ZD test results

Exp. No	1	2	3	4	5	6	7	8	9
Parent metal (Hv)	293	315	309	321	277	326	360	311	325
WA (Hv)	283	280	287	302	291	302	303	305	297
ZD (Hv)	277	279	282	283	283	288	283	289	289

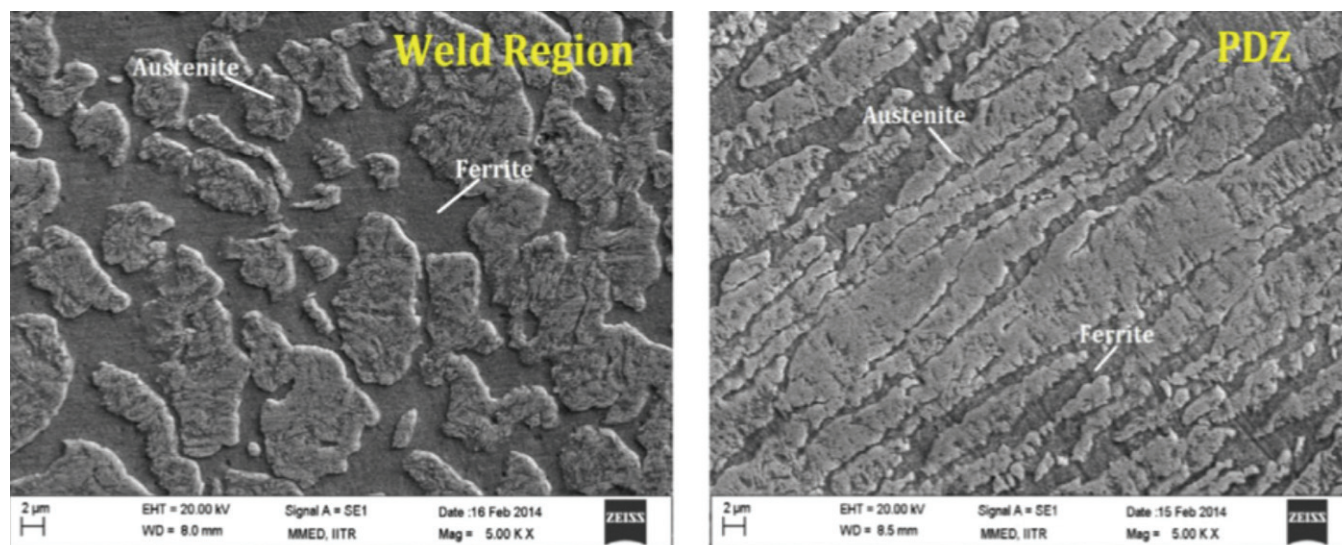


Figure 13: SEM pictures of the weld area

welding. The rotating component’s surfaces that were parallel to the friction surfaces received loading—that is, pressure—applied in a direction perpendicular to the friction surface. In keeping with the actual method, the loading was delivered in two steps. Parts are believed to be in touch at first. The heat loss from convection, conduction, and radiation were taken into account in thermal boundary conditions.

Metallographic Analysis

Three different zones – the weld area (WA), the zone with some deformation (ZD), and the base substance – were discovered by micro structural analyses of the weld (BM). The welding upset pressure has an impact on the three separate zones’ sizes. Very small grains that form in the weld region as a result of dynamic recrystallization in the area are distinctive. The heat-affected zone known as the partially deformed zone experiences slightly less distortion than the weld region. The majority of the components, which contribute to the basic material’s microstructure, are unaffected. Figure 14 displays the SEM pictures of the experiment’s PDZ and weld region. It is evident that austenite has developed in the matrix of ferrite. For the experiments, the XRD patterns were plotted. The experiment’s XRD plot is displayed in Figure 14.

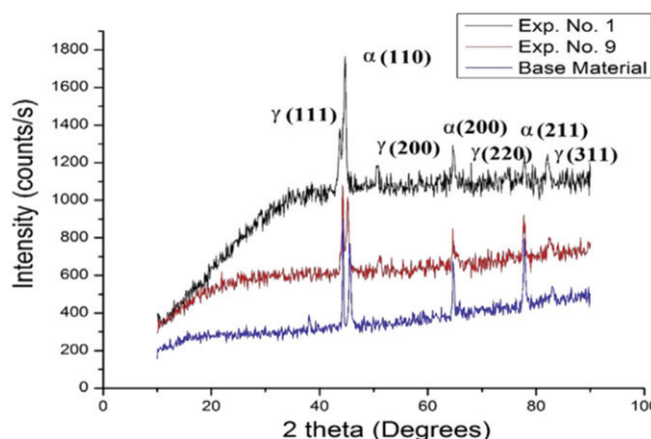


Figure 14: XRD Experiment Plot

Micro hardness

Micro hardness tests were successfully done to examine the differences in hardness in the base substance (B.S), zone with some deformation (ZD), and weld area (WA). Table 7 provides the combined results.

Figure 15 makes it evident that the welded materials’ hardness is higher near the interface than it is in the PDZ. Analysis reveals that the heat-affected zones’ hardness was lower than that of the underlying material.

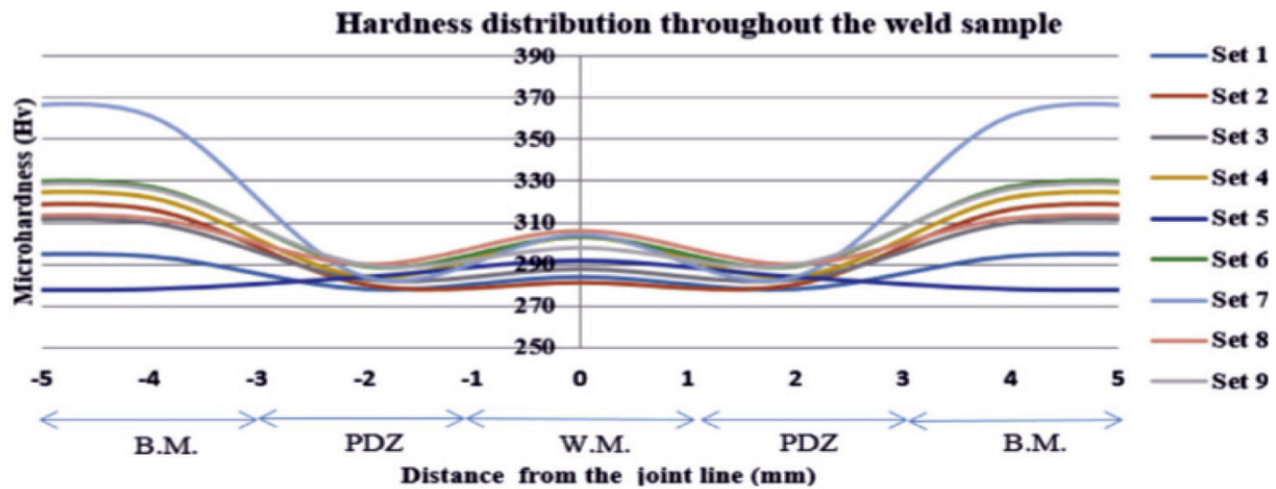


Figure 15: Distribution of micro hardness in the weld sample under consideration

SA213 Tube to SA387 tube plate materials

By employing an outside tool to friction weld tube to tube plate, leak-proof, high-quality junctions with high mechanical standards can be created. Friction welding is used to join SA 213 tube and SA 387 tee l plate made of two dissimilar materials using three distinct filler materials. Steel balls, filler plate, and brass sheet make up the filling substances. The flow of metal pattern toward the centre of the device axis is improved and validated using an external tungsten carbide tool. Micro structural investigations disclose the position and the flow of metal toward the centre of the work item. The test for hardness that follows makes a high hardness value certain at the welded area establishes the metal moving through the centre of the pit has a powerfully bonded structure. Using a tungsten carbide external tool, influence of temperature and examining the friction created in the tube to tube plate during the friction welding procedure. In the review work, SA 213 tube and SA 387 tube plate were connected using two different methods: with hole [WH] and without hole [WOH].

FWTPET Method

Vertical milling machines are used to perform the friction welding process. Strong weld joints are produced using the FWTPET technique [7]. The FWTPET machine is made up of a tool holder, spindle, table, and a supporting framework. With the aid of a backing block, the tube is fitted and assembled to clamp in the machine-wise. Specific setting conditions have been provided for each work piece, and an appropriate quantity of value is offered as the input parameters. The required hole dimension is then drilled at the centre of the tube plate. The tool is designed to move downward toward the top surface of the work piece, providing the required

depth of cut and feed. Due to the tool's rotating force, there will be friction between the tool and the workpiece. Between these materials is where the heat is produced.

6.0 Conclusion

Thus, a review of the FSW (friction stir welding) procedure used to weld different materials is carried out. As a result, their microstructure and mechanical characteristics are effectively reviewed and tallied. Al6061 alloy, UNS S31803 stainless steel, friction Al7075 alloy, and SA213 tube to a tube plate SA 387 microstructure and mechanical properties are evaluated and compiled along with their experimental setups.

References

- [1] Rajamadam, (2016): "Experimental and Numerical Investigation of AL 6061 Alloys Reinforced with SiC-TiO₂" *International Journal of Mechanical and Production Engineering*, Volume- 4, Issue-11.
- [2] Ashok Kr. Mishra, (2012): "Tribological Behaviour of Al-6061 / SiC Metal Matrix Composite by Taguchi's Techniques" *International Journal of Scientific and Research Publications*, Volume 2, Issue 10.
- [3] Naik Sachin Ashok, (2016): "Investigation on Mechanical and Tribological Properties of 6061 Aluminium – SiC Alloy Fabricated by Stir Casting Method and Equal Channel Angular Extrusion: The Review" *International Research Journal of Engineering and Technology (IRJET)*, Volume: 03 Issue: 04.
- [4] S. Suresh Kumar, (2014): "Influence of Residual Stress on Stress Intensity Factor Estimation of Multiple

- Cracks in a Dissimilar Welded Joint” 1st International Conference on Structural Integrity, *Procedia Engineering* 86 (2014) 234 – 241.
- [5] Mr. P H Shah, (2016): “An experimental investigation of temperature distribution and joint properties of Al 7075 T651 friction stir welded aluminium alloys” 3rd International Conference on Innovations in Automation and Mechatronics Engineering, *Procedia Technology* 23 (2016) 543 – 550.
- [6] Mohammed Asif. M, (2015): “Finite element modelling and characterization of friction welding on UNS S31803 duplex stainless steel joints” *Engineering Science and Technology*, an International Journal, Issue:1-9.
- [7] S.Pandiyarajan, (2017): “An Investigation of metal flow during friction welding of SA213 to SA387 tube plate with Backing Block” *International Research Journal of Engineering and Technology* issue: 05.
- [8] G. Elatharasan, (2013): “An experimental analysis and optimization of process parameter on friction stir welding of AA 6061-T6 aluminum alloy using RSM” International Conference on Design and Manufacturing, *Procedia Engineering* 64 (2013) 1227 – 1234.
- [9] Miller, (2016): “Probability and statistics for engineers” *International Journal of Mechanical and Production Engineering*, issue:5
- [10] Wang, (2014): “Modeling of continuous drive friction welding of mild steel” *International Research Journal of Engineering and Technology*, issue:10.
- [11] MuthuMekala N, Balamurugan C, Bovas Herbert Bejaxhin, “Deform 3D Simulation and Experimental Investigation of Fixtures with Support Heads”, *MECHANIKA*. 2022 Volume 28(2): 130"138, ISSN 1392"1207. <http://dx.doi.org/10.5755/j02.mech.29468>.
- [12] A. Bovas Herbert Bejaxhin, G.M. Balamurugan, S.M. Sivagami, K. Ramkumar, V. Vijayan and S. Rajkumar, “Tribological Behaviour and Analysis on Surface Roughness of CNC Milled Dual Heat Treated Al6061 Composites”, *Advances in Materials Science and Engineering*, Volume 2021, Article ID 3844194, 14 pages, <https://doi.org/10.1155/2021/3844194>.
- [13] J Jones Praveen, M Vinosh, A Bovas Herbert Bejaxhin, G Paulraj, “Embedded effect of ZrB2-Si3N4 on tribologicalbehaviour of Al 8011 metal matrix composite”, *Materials Today: Proceedings*, Elsevier. <https://doi.org/10.1016/j.matpr.2020.10.954>.
- [14] VasudevaRao, P. Periyaswamy, A. Bovas Herbert Bejaxhin, E. Naveen, N. Ramanan, and Aklilu Teklemariam, *Wear Behavioural Study of Hexagonal Boron Nitride and Cubic Boron Nitride-Reinforced Aluminum MMC with Sample Analysis*, Hindawi, *Journal of Nanomaterials*, Volume 2022, Article ID 7816372, 10 pages, <https://doi.org/10.1155/2022/7816372>.
- [15] L. Natrayan, M. Ravichandran, DhinakaranVeeman, P. Sureshkumar, T. Jagadeesha, R. Suryanarayanan, WubishetDegifeMammo, “Enhancement of Mechanical Properties on Novel Friction Stir Welded Al-Mg-Zn Alloy Joints Reinforced with Nano-SiC Particles”, *Journal of Nanomaterials*, vol. 2021, pp. 1-10, 2021. <https://doi.org/10.1155/2021/2555525>
- [16] L.Natrayan, V. Sivaprakash and M. S. Santhosh. “Mechanical, Microstructure and wear behaviour of the material AA6061 reinforced SiC with different leaf ashes using advanced stir casting method.” *International Journal of Engineering and Advanced Technology*, vol. 8, pp. 366-371, 2018
- [17] L.Natrayan, M. S. Santhosh, R. Mohanraj, and R. Hariharan. “Mechanical and Tribological Behaviour of Al₂O₃ & SiC Reinforced Aluminium Composites Fabricated via Powder Metallurgy”. *IOP Conf. Ser. Mater. Sci. Eng*, vol. 561, no. 1, pp. 012038, 2019.